The Journal of Neuroscience, July 1, 1999, *19*(13):5348–5359

The *Caenorhabditis elegans unc-49* Locus Encodes Multiple Subunits of a Heteromultimeric GABA Receptor

Bruce A. Bamber,[3] Asim A. Beg,[1] Roy E. Twyman,[2] and Erik M. Jorgensen[3]

[1]*Interdepartmental Program in Neuroscience and Departments of* [2]*Neurology and* [3]*Biology, University of Utah, Salt Lake City, Utah 84112*

Ionotropic GABA receptors generally require the products of three subunit genes. By contrast, the GABA receptor needed for locomotion in *Caenorhabditis elegans* requires only the *unc-49* gene. We cloned *unc-49* and demonstrated that it possesses an unusual overlapping gene structure. *unc-49* contains a single copy of a GABA receptor N terminus, followed by three tandem copies of a GABA receptor C terminus. Using a single promoter, *unc-49* generates three distinct $GABA_A$ receptor-like subunits by splicing the N terminus to each of the three C-terminal repeats. This organization suggests that the three UNC-49 subunits (UNC-49A, UNC-49B, and UNC-49C) are coordinately rescued and therefore might coassemble to form a heteromultimeric GABA receptor. Surprisingly, only UNC-49B and UNC-49C are expressed at high levels, whereas UNC-49A expression is barely detectable. Green fluorescent protein-tagged UNC-49B and UNC-49C subunits are coexpressed in muscle cells and are colocalized to synaptic regions. UNC-49B and UNC-49C also coassemble efficiently in *Xenopus* oocytes and HEK-293 cells to form a heteromeric GABA receptor. Together these data argue that UNC-49B and UNC-49C coassemble at the *C. elegans* neuromuscular junction. Thus, *C. elegans* is able to encode a heteromeric GABA receptor with a single locus.

Key words: GABA neurotransmission; GABA receptor; C. elegans*; unc-49; coordinate regulation of subunit expression; GABA receptor diversity; GABA receptor structure–function*

Vertebrate genomes encode at least 14 different $GABA_A$ receptor subunits, which fall into the α, β, γ, δ, or ϵ classes. $GABA_A$ receptor subunits belong to the ligand-gated ion channel superfamily (for review, see Macdonald and Olsen, 1994), and all share a highly conserved overall structure. The N terminus consists of a large extracellular domain containing a pair of disulfide-bonded cysteines separated by 13 amino acids and four peptide loops that are thought to form the ligand-binding site (for review, see Galzi and Changeux, 1994). The remainder of each subunit consists of four transmembrane domains designated M1 through M4. The M2 domain forms the channel pore, and the intracellular loop between M3 and M4 contains regulatory phosphorylation sites plus domains possibly involved in localization of the subunit to synapses (Olsen and Tobin, 1990; Meyer et al., 1995; Moss and Smart, 1996). $GABA_A$ receptor subunits coassemble to form pentameric ligand-gated chloride channel receptors. These receptors play a key role in inhibitory neurotransmission in the brain.

$GABA_A$ receptors usually contain subunits of three different classes. Thus, the vertebrate genome potentially could produce thousands of $GABA_A$ receptor subtypes by assembling receptors with different subunit composition and stoichiometry. However, histochemical studies of the brain indicate that neurons express specific combinations of subunit genes, suggesting that the number of $GABA_A$ receptor subtypes is constrained by subunit expression patterns. Immunoprecipitation studies have confirmed this view, because fewer than a dozen major $GABA_A$ receptor subtypes have been demonstrated experimentally (McKernan and Whiting, 1996). Thus, the formation of $GABA_A$ receptors seems to be a highly regulated process, and neurons are able to define the complement of $GABA_A$ receptors on postsynaptic and extrasynaptic membranes precisely (Nusser et al., 1998).

The regulatory mechanisms by which neurons populate synapses with the correct $GABA_A$ receptor subtypes are not well understood. How is subunit expression coregulated such that the appropriate combinations of subunits are produced? How are subunits assembled in the correct stoichiometry? How are they localized to the appropriate synapses?

To answer these and other questions, we are undertaking a comprehensive study of GABA neurotransmission in the nematode *Caenorhabditis elegans* (McIntire et al., 1993a). Mutants lacking GABA neurotransmission display a characteristic locomotory defect referred to as the "shrinker" phenotype, which arises from the loss of inhibitory input to body wall muscles (McIntire et al., 1993b). One shrinker mutant, *unc-49*, is resistant to the paralyzing effects of the $GABA_A$ receptor agonist muscimol, suggesting that *unc-49* is necessary for GABA receptor function (McIntire et al., 1993a). Here, we demonstrate that *unc-49* encodes the GABA receptor that functions at inhibitory neuromuscular synapses. *unc-49* possesses an unusual overlapping gene structure that generates three distinct ligand-gated ion channel subunits under the control of a single promoter. Two of these

Received Dec. 31, 1998; revised March 22, 1999; accepted April 13, 1999.

This work was supported by National Institutes of Health Grants NS34307 (E.M.J.) and NS31519 (R.E.T.) and the Klingenstein Fund. We thank A. M. L. McClellan for single-channel recordings; J.-L. Bessereau for integrating transgene constructs; Y. Jin and H. R. Horvitz for supplying the *unc-49(n2392)* allele; the *Caenorhabditis* Genetics Center for strains; M. Metzstein for assistance with Genefinder predictions; D. P. Morse for the gift of *C. elegans* RNA; R. Shapiro for suggestions regarding PCR analysis of bacterial colonies; R. Barstead and P. Okkema for *C. elegans* cDNA libraries; E. Kofoid and S. Bibikov for help with the GCG sequence analysis package; D. Grimes for assistance with *Xenopus* oocytes; and S. Mango, V. Maricq, and members of the Jorgensen and Twyman labs for critical reading and helpful discussion. GenBank accession numbers: AF151640 (UNC-49A), AF151641 (UNC-49B.1), AF151642 (UNC-49B.2), AF151643 (UNC-49B.3), AF151644 (UNC-49C), and AF151645 (UNC-49C short).

Correspondence should be addressed to Dr. Erik M. Jorgensen, Department of Biology, University of Utah, 257 South 1400 East, Salt Lake City, UT 84112-0840.

Dr. Twyman's present address: R. W. Johnson Pharmaceutical Research Institute, 920 Route 202 South, Raritan, NJ, 08869.

subunits are coexpressed in muscle cells, are colocalized to synaptic regions, and coassemble to form a heteromeric GABA receptor. Thus, the *unc-49* locus coordinately regulates the expression of multiple-coassembling GABA receptor subunits.

MATERIALS AND METHODS

C. elegans *strains*

unc-49 strains and corresponding alleles used in this study are as follows: CB382 *unc-49(e382) III*, CB407 *unc-49(e407) III*, EG1232 *unc-49(e468) III*, CB641 *unc-49(e641) III*, CB929 *unc-49(e929) III*, MT2976 *unc-49(n1324) III*, MT3123 *unc-49(n1324n1345) III*, and MT6224 *unc-49(n2392) III*. MT6225 *unc-49(n2393) III* is likely to be a re-isolate of *n2392* because the mutations are identical. The *n1324* allele was isolated from MT2879, in which Tc1 transposons are active. *n1345* is a revertant of this allele. The preceding list represents all *unc-49* alleles isolated to date.

C. elegans *transformation*

Transformation was performed by microinjection of plasmid and cosmid DNA into the *C. elegans* germline (Mello et al., 1991). T21C12 and T21C12ΔMlu were injected at 80 ng/μl into *unc-49(e382); lin-15(n765ts)*. pEK1, a plasmid that contains the wild-type *lin-15* gene (Clark et al., 1994; S. G. Clark and X. Lu, personal communication), was coinjected at 80 ng/μl as a cotransformation marker. Progeny of injected animals were raised at the restrictive temperature for *lin-15(n765ts)*, and successfully transformed animals were recognized by their non-Muv phenotype.

T21C12 and T21C12ΔMlu contain only 290 base pairs upstream of the start codon. These plasmids were able to rescue the strong shrinker phenotype of *unc-49*, but they were incapable of complete rescue. Transformed animals could not move in a straight line. Instead, they curved dorsally, suggesting an overexpression of GABA receptors on the ventral side relative to the dorsal side. Complete rescue was obtained by coinjecting two overlapping linear DNA fragments that recombined in the germline to form the complete *unc-49* locus with an additional 4 kb of 5′ flanking DNA. One fragment was a genomic PCR fragment containing the 4 kb 5′ flanking DNA and 4 kb of the 5′ end of the T21C12 insert (amplified with primers 40 and 110). The other fragment was a gel-purified *Spe*I–*Mlu*I fragment of T21C12. The overlap between these two fragments was 970 bases. Fragments were injected at ~10 ng/μl each, along with 40 ng/μl pEK1 and 40 ng/μl 1 kb ladder (Life Technologies, Gaithersburg, MD). Transformed animals from these injections were fully rescued. This method was used because constructs containing the 4 kb of 5′ flanking DNA were unstable and could not be maintained in bacterial hosts.

In experiments to determine which of the *unc-49* open reading frames is required for the rescue of *unc-49(e382)*, the UNC-49A open reading frame was disrupted by Klenow-filling the *Nde*I site near the UNC-49A M3 domain, the UNC-49B open reading frame was disrupted by Klenow-filling the unique *Bsi*WI site, and the UNC-49C open reading frame was disrupted by deleting a fragment between two *Nru*I sites, which included all of the UNC-49C M1 domain.

cDNA analysis

This section is an overview of the experiments that led to the isolation of UNC-49A, UNC-49B, UNC-49C, and UNC-49Cshort cDNA clones. These experiments also rule out the possibility of splicing between the C-terminal repeats to produce chimeric subunits derived from more than one C-terminal repeat (for example, such a chimeric subunit might contain M1 and M2 of UNC-49A and M3 and M4 of UNC-49B). Below is a description of the large number of clones that were examined, which allowed us to conclude that no chimeric subunits are produced.

UNC-49A. The first UNC-49A cDNA clones were isolated from the cDNA library supplied by P. Okkema (University of Illinois at Chicago, Chicago, IL), probed with a mixture of labeled PCR fragments generated using primers 7 (corresponding to the conserved disulfide-bonded loop) and 8 (corresponding to repeat A, M4), and primers 5 (repeat B, M1) and 6 (repeat B, M4). Four partially spliced UNC-49A cDNA clones were isolated. We then performed an RT-PCR experiment to isolate additional UNC-49A clones. We used first-strand cDNA, which was prepared using poly(A^+)-selected *C. elegans* RNA (see Preparation of First-Strand cDNA below). PCR was performed in two rounds. In the first round, primer 68 (conserved N-terminal domain) was paired with primer 93 (repeat A, M4). This reaction produced a product of ~1 kb that was cloned with the TA cloning kit (Invitrogen, San Diego, CA). One microliter of this reaction was reamplified using the nested primers 73 and 94. This reaction produced an abundant 1 kb product that was likewise TA-cloned. Colonies from both ligations were analyzed by colony hybridization, using the partial UNC-49A cDNA isolated above; 96 positive colonies were picked and analyzed by double digestion with *Rsa*I and *Not*I restriction enzymes (Life Technologies). This combination of enzymes produces a "fingerprint" restriction pattern that allows for the rapid screening of large numbers of clones and, therefore, the detection of rare clones of unusual structure. Based on unique restriction patterns, 14 clones were sequenced, and five of these corresponded to fully spliced UNC-49A mRNA. Six of the remaining clones contained unspliced introns or aberrant splice patterns that interrupted the UNC-49A open reading frame, two clones contained internal deletions, and one clone contained non-*unc-49* sequences.

UNC-49B. Three UNC-49B cDNA clones were isolated from the cDNA library provided by R. Barstead (Oklahoma Medical Research Foundation, Oklahoma City, OK). Two of these clones were identical and therefore probably not independent. Additional UNC-49B cDNA clones were isolated in two RT-PCR experiments. In the first, first-strand cDNA was prepared from total *C. elegans* RNA amplified as described for UNC-49A, using primers 5 (repeat B, M1) and 6 (repeat B, M4). Seventeen clones with inserts were analyzed further by double digesting with *Rsa*I and *Not*I restriction enzymes (Life Technologies). Using these enzymes, we were able to discriminate among the three UNC-49B isoforms. This analysis showed that 7 of 17 corresponded to UNC-49B.1, 9 of 17 corresponded to UNC-49B.2, and 1 of 17 corresponded to UNC-49B.3. In the second RT-PCR experiment, first-strand cDNA prepared with poly(A^+)-selected *C. elegans* RNA was amplified by using primers 68 and 74 (repeat B, M4), SL1/74, and SL2/74 (see Fig. 2). Next, 1 μl of each reaction was reamplified in a second round of PCR reactions, using the nested primer pairs 73/6, SL1/6, and SL2/6. Each of these reactions produced plainly visible bands when analyzed by agarose gel electrophoresis, and reaction products were cloned with the TA cloning kit (Invitrogen). Transformations were analyzed by colony hybridization (Ausubel et al., 1995), using Duralon nylon filters (Stratagene, La Jolla, CA). An UNC-49B cDNA fragment was used as a probe after it had been gel-purified away from vector sequences with the QIAquick Gel Extraction Kit (Qiagen, Valencia, CA) and labeled by random priming (specific activity $>1 \times 10^8$ cpm/μg). Positive colonies were identified by a Phosphorimager (Applied Biosystems, Foster City, CA), and 9–10 positive colonies were picked from each plate (The SL2/6 PCR reaction was performed twice, and a total of nine positive colonies were picked from these two trials). Then each clone was subjected to double digestion with *Rsa*I and *Not*I restriction enzymes, and clones with unique restriction patterns were identified. Those clones with unique restriction patterns were sequenced. We isolated two UNC-49B.1 clones and one UNC-49B.2 cDNA clone. The combinations of primers used in this section would be able to detect chimeric subunits, had they been present.

UNC-49C. The isolation of UNC-49C and UNC-49B cDNA clones was performed simultaneously. Only details specific to the isolation of UNC-49C clones are noted here. Two independent UNC-49C cDNA clones were isolated from the library supplied by R. Barstead. RT-PCR analysis of total *C. elegans* RNA was performed by using primers 1 (N terminus of repeat C) and 4 (repeat C, M4). Fourteen clones contained inserts that represented a single size class. One of these was sequenced and found to correspond to the UNC-49C splicing pattern. RT-PCR of poly(A^+)-selected *C. elegans* RNA was performed as described for UNC-49B, using primers 75 (repeat C, M4) and 4. We sequenced two UNC-49C cDNA clones isolated in this experiment. The combinations of primers used to detect UNC-49C clones also should have been able to detect chimeric subunits, if they were present.

UNC-49Cshort. Nine UNC-49Cshort clones were isolated from the cDNA library supplied by R. Barstead. The RT-PCR analysis of poly(A^+)-selected *C. elegans* RNA described above should have detected UNC-49Cshort mRNA had it contained trans-spliced SL1 or SL2 leader sequences. We did not isolate SL-spliced UNC-49Cshort cDNA clones. However, we isolated other cDNA clones in which SL1 or SL2 sequences were spliced to internal introns. Because such splices are likely to be rare splicing errors, our protocols appear to be very sensitive. Thus the absence of SL1 or SL2 product indicates that these are not normally produced.

Summary statistics. Twenty-three cDNA clones that corresponded to *unc-49* sequences were isolated from the library supplied by R. Barstead, and 14 were of sufficient length that they could be grouped into the UNC-49B, UNC-49C, or UNC-49Cshort class. Ninety-six clones were

isolated in the RT-PCR analysis of total *C. elegans* RNA, and 175 clones were isolated in the RT-PCR analysis of poly(A^+)-selected *C. elegans* RNA. Ninety-six of these were generated by UNC-49A-specific primers; 16 of these clones were sequenced. Seventy-nine clones were generated by primers specific for UNC-49B and UNC-49C; 18 of these 79 clones were sequenced. Because multiple clones of most splice variants were isolated, we believe that this analysis was sufficiently thorough to provide a complete picture of the *unc-49* splicing pattern.

Polymerase chain reaction

Reactions were performed by using the PTC-100 or PTC-200 thermal cyclers (MJ Research, Cambridge, MA). We used either *Taq* DNA polymerase (Life Technologies) or the Expand Long Template PCR system (Boehringer Mannheim, Indianapolis, IN). Primer sequences are as follows (each primer number is in bold type): **1**, atg tgt tca gat gcg tat tcg; **4**, gat gaa aac aag agg aaa gcg; **5**, ctg atc gtc acc ata tct tgg; **6**, aag aca atg gga aac cgt atc; **7**, tgt cca atg gac ctg aag ctg; **8**, cgg cgt att cta gaa gtg aac; **19**, tgg agc ccg tca gta tcg gcg; **20**, gta gcg acc ggc gct cag ctg; **37**, atc ccc agc gcc tcc ccg tta; **38**, ttt ttg cct gtt ttt gtc gcc; **39**, ata gtc ata aat gga ccc gcg; **40**, ctc gga aat aat gtg cat gaa; **41**, ttc aca cat ggt gca tcg aag; **42**, gct agt gtg ata agt gct gtg; **45**, cga ttt tct cag tat gca cgg; **46**, att ttc gca cca cac ctt ctc; **47**, tat gtc gca aaa ttc gac gcc; **48**, gat gaa gtg ctg gca agt gtc; **68**, cac att aga ctt cta cat gcg; **73**, aaa cgt ggc aag acc ctc gac; **74**, cca gta gac tat att gaa gat; **75**, agc cag aag aga gtg ttg aac; **83**, ata cca tca tga agc aga cac; **93**, atg aag tag gcc cag tag ccg; **94**, gta gcc gac gtt gaa gag cac; **110**, atg gtg gtt ttg ttc ccc tcc; **SL1**, ggt tta att acc caa gtt tga g; **SL2**, ggt ttt aac cca gtt act caa g; **M13F**, cgc cag ggt ttt ccc agt cac gac; **M13R**, tca cac agg aaa cag cta tga c.

Library screening

Two different cDNA libraries were screened. The first, prepared by using poly(A^+) *C. elegans* RNA and the λZap vector (Stratagene), was a kind gift of Dr. R. Barstead (Barstead and Waterston, 1989). This library (350,000 plaques) was screened with Duralon nylon filters (Stratagene) according to the manufacturer's instructions, using three PCR products approximately corresponding to the transmembrane domains of C-terminal repeat A, B, and C as probes. These fragments were generated by using primer pairs 7 and 8, 5 and 6, and 1 and 4, respectively. Probes were labeled to $>1 \times 10^8$ cpm/μg by random priming and combined in equal amounts in the hybridization mixture. Inserts from positive clones were excised by using the ExAssist helper phage/SOLR strain system (Stratagene).

The second library, prepared from oligo U-selected *C. elegans* mRNA and the λGT11 vector, was kindly supplied by Dr. P. Okkema (Okkema and Fire, 1994). This library (400,000 plaques) was screened as described above, except that the C-terminal repeat C probe was omitted. Inserts from positive clones were PCR-amplified with primers 19 and 20 and cloned with the TA cloning kit (Invitrogen). Growing and plating of recombinant phage and the identification of positive plaques were performed according to standard techniques (Ausubel et al., 1995).

Preparation of first-strand cDNA

First-strand cDNA was prepared in two different ways. First, total *C. elegans* RNA (D. P. Morse, University of Utah, Salt Lake City, UT) was reverse-transcribed by using oligo-dT primers (12–18 nucleotides in length) and Superscript II reverse transcriptase (Life Technologies), according to the protocol supplied with the enzyme. Second, *C. elegans* RNA (D. P. Morse) first was poly(A^+)-selected, using Dynabeads oligo-dT_{25} (Dynal, Lake Success, NY), and then reverse-transcribed (Rodriguez et al., 1994).

Northern analysis

N2 worms were grown on plates containing 2% agarose (FMC Bioproducts, Rockland, ME), and RNA was isolated via the direct phenol extraction method (Andres and Thummel, 1994). Poly(A^+) RNA was purified from total RNA (75 μg per lane), using Oligo-dT Dynabeads (Dynal) according to the manufacturer's instructions, and eluted directly into Northern loading buffer. Samples were run on a 1.2% formaldehyde-containing MOPS/EDTA agarose gel and transferred to Zeta-probe nylon membranes (Bio-Rad, Hercules, CA) by capillary transfer, using standard techniques (Ausubel et al., 1995). Blots were probed with labeled cDNA fragments ($>10^8$ cpm/μg), which specifically hybridized to the UNC-49A (*Rsa*I–*Eco*RI fragment of the 7/8 PCR fragment), UNC-49B (5/6 PCR fragment), and UNC-49C (1/4 PCR fragment) mRNAs. Blots were reprobed with an *act-1* probe (M. Horner, University of Utah, Salt Lake City, UT) to normalize *unc-49* signals for variations in RNA loading and transfer. Band intensity was quantified with a Phosphorimager (Applied Biosystems).

Computer sequence analysis

Multiple sequence alignments were performed with the Pileup program in the Genetics Computer Group software package, version 9.0. Sequences used in the alignment (and their accession numbers) are listed as follows: rat $GABA_A$ receptor subunits α1 (SwissProt: p18504), α2 (SwissProt: p23576), α3 (SwissProt: p20236), α4 (SwissProt: p28471), α5 (SwissProt: p19969), α6 (SwissProt: p30191), β1 (SwissProt: p15431), β2 (SwissProt: p15432), β3 (SwissProt: p15433), γ1 (SwissProt: p23574), γ2 (SwissProt: p18508), γ3 (SwissProt: p28473), δ (SwissProt: p18506); rat $GABA_C$ receptor subunits ρ1 (SwissProt: p50572), ρ2 (SwissProt: p47742), ρ3 (SwissProt: p50573); rat glycine receptor subunits α1 (SwissProt: p07727), α2 (SwissProt: p22771), α3 (SwissProt: p24524), β (SwissProt: p20781); human $GABA_A$ receptor ϵ subunit (GenBank: U66661); *Drosophila melanogaster rdl* gene product (SwissProt: p25123); *Drosophila* GABA receptor β-subunit (SwissProt: q08832); *lymnaea stagnalis* GABA receptor β-subunit (SwissProt: p26714); and avermectin-sensitive glutamate-gated chloride channel α1-subunit (pir2: s50864), α2B-subunit (DDBJ/EMBL/GenBank: AJ000537) β-subunit (GenBank: U14525). Alignments were performed with full-length subunits. Alignments of representative GABA receptor subunits used to establish the conservation shown in Figure 3*B* were performed by using the Clustal alignment method within the MegAlign program of the DNAstar sequence analysis package (DNAstar, Madison, WI). The rat α1, β1, γ1, δ, and ρ1 GABA receptor subunits, the human ϵ1 GABA receptor subunit, and *Drosophila rdl* protein were used for this alignment. Signal peptide cleavage sites were predicted with the PSORT program (K. Nakai, Osaka University, Japan). Consensus phosphorylation sites were identified with the PPSearch program (European Molecular Biology Laboratory data library).

Genomic Southern blot analysis

The preparation of genomic DNA and Southern blot analysis were performed according to standard techniques (Ausubel et al., 1995), using Zeta-probe nylon membranes (Bio-Rad). Blots were probed with a mixture of three labeled fragments: (1) an *Eco*RI fragment that includes bases 1043–2983 of T21C12, (2) a genomic PCR product (see Polymerase Chain Reaction in Materials and Methods) generated by using primers 7 and 8 (see Fig. 2*A*), and (3) a second *Eco*RI fragment that includes bases 8968–12054 of T21C12. Each fragment was labeled by random priming (Feinberg and Vogelstein, 1983) to a specific activity of $>10^8$ cpm/μg. Prehybridization, hybridization, and washing (high stringency) were performed according to the manufacturer's instructions. Blots were visualized by autoradiography or by using a Phosphorimager (Applied Biosystems).

DNA sequencing

Sequencing of cDNA clones was performed with an Applied Biosystems automated DNA sequencing apparatus at the Sequencing Core Facility, University of Utah. Genomic sequencing was performed on genomic PCR fragments corresponding to UNC-49B by using the ThermoSequenase cycle sequencing kit (Amersham Pharmacia, Piscataway, NJ).

Green fluorescent protein (GFP) constructs

The S65C variant of GFP containing three introns (1997 Fire vector kit) was cloned into the T21C12ΔMlu construct such that GFP was inserted, in frame, into the large intracellular loop of one subunit, whereas the other subunits were wild type. UNC-49A was tagged by inserting a Klenow-filled *Eco*RV to *Xba*I fragment of pPD103.87 into a T4 DNA–polymerase-treated *Bsm*I site. UNC-49B was tagged by inserting a Klenow-filled *Cla*I to *Bam*HI fragment of pPD102.33 into a *Bsa*BI site. UNC-49C was tagged by inserting a Klenow-filled *Cla*I to *Not*I fragment of pPD103.87 into a T4 DNA–polymerase-treated *Bsm*I site. To tag the putative UNC-49Cshort subunit specifically, we Klenow-filled the *Spe*I site within the common N terminus in the UNC-49C-tagged construct. To generate transgenic lines expressing the GFP-tagged subunits, we injected *unc-49(e382); lin-15(n765ts)* worms with linear fragments of the GFP-tagged constructs and genomic PCR fragments containing 5′ flanking DNA as described above. A slight variation was used to generate UNC-49B::GFP and UNC-49Cshort::GFP lines. Instead of coinjecting a *Spe*I–*Mlu*I *unc-49* fragment with a 110/40 genomic PCR product, we

coinjected an *Afl*II–*Mlu*I *unc-49* fragment with a 110/38 genomic PCR fragment. This pair of fragments contained 450 base pairs of overlapping DNA. As a control, the *Afl*II–*Mlu*I fragment of the unmodified T21C12 cosmid was injected with, and without, the 5′ genomic fragment; rescue of *unc-49* required the 5′ genomic fragment. Our original rescue experiments suggested that elements required for dorsal expression are contained within the 4 kb of 5′ flanking DNA. We confirmed this observation by injecting the UNC-49B::GFP and UNC-49C::GFP constructs as circular cosmids without the 4 kb of 5′ flanking DNA. Transformants from these injections showed much stronger GFP fluorescence in the ventral cord than in the dorsal cord.

Electrophysiology

Two-electrode voltage-clamp electrophysiology was performed on *Xenopus laevis* ooctyes injected with cRNA encoding UNC-49B or UNC-49C subunits. cRNA was prepared with the the mMessage mMachine kit (Ambion, Austin, TX). Recordings were performed and analyzed as described in Donevan et al. (1998). All combinations of subunits were tested in parallel in at least two independent experiments (at least four oocytes for each combination of mRNAs per experiment). The absolute values for the GABA EC_{50} and Hill number were somewhat variable; however, within any given experiment the incorporation of UNC-49C consistently resulted in a significantly higher EC_{50} and a significantly lower Hill number. Single-channel recordings were performed as described in Lavoie et al. (1997) except that 1 mM GABA was applied continuously. Single-channel conductance was determined by fitting Gaussian curves to all points histograms.

RESULTS

Structure of the *unc-49* locus

We cloned *unc-49* by using standard microinjection rescue techniques (Mello et al., 1991). Genetic map data indicated that *unc-49* was located on chromosome III between *lin-19* and *mel-23*. One cosmid in this region, T21C12, contained a predicted 12 kb open reading frame (T21C12.1) with significant similarity to $GABA_A$ receptor subunits (Wilson et al., 1994). This cosmid was injected into *unc-49(e382)* animals, and two stable lines were established that rescued the *unc-49* shrinker phenotype. A construct containing only the T21C12.1 open reading frame (T21C12ΔMlu) also rescued the *unc-49* shrinker phenotype (data not shown). Both T21C12 and T21C12ΔMlu contained only 290 nucleotides 5′ of the predicted start codon, and both constructs only partially rescued the *unc-49* locomotion defect. Complete rescue required the addition of 4 kb of 5′ flanking DNA (see Materials and Methods). We confirmed that the T21C12.1 open reading frame corresponded to the *unc-49* gene by demonstrating that all *unc-49* mutations were contained within T21C12.1 (see below).

The structure of the *unc-49* locus is very different from a typical ligand-gated ion channel subunit gene. At its 5′ end *unc-49* contains a single region encoding the N-terminal half of a GABA receptor subunit. The rest of the locus is made up of three repeated regions, designated A, B, and C, each encoding the C-terminal half of a subunit (Fig. 1*A*). The N-terminal region encodes most of the extracellular residues, including two of the four loops thought to form the ligand-binding site (Galzi and Changeux, 1994) and the absolutely conserved disulfide-bonded loop. Each of the three repeated 3′ regions encodes the other two putative ligand-binding loops, corresponding to the BDI and BDII GABA-binding domains identified by Amin and Weiss (1993, 1994), and all four membrane-spanning domains.

The *unc-49* locus encodes three distinct subunits

We analyzed the structures of the mRNAs produced from *unc-49* and demonstrated that *unc-49* is a compound locus that produces multiple receptor subunits. Three full-length subunits, UNC-49A, UNC-49B, and UNC-49C, are generated by splicing the exons encoding the N-terminal half of a subunit to the exons encoding the C-terminal repeats A, B, and C, respectively (Fig. 1*B*).

UNC-49A

RT-PCR experiments generated multiple partial cDNA clones corresponding to the fully spliced UNC-49A mRNA. Screening cDNA libraries yielded a few UNC-49A cDNA clones, but all of these contained unspliced introns that introduced premature stop codons.

UNC-49B

Multiple isoforms of UNC-49B mRNAs were identified. Two isoforms encode identical full-length UNC-49B subunits, but they differ at their 3′ ends (one UNC-49B isoform contains the UNC-49C exons in its 3′ untranslated region). Alternative splicing within the UNC-49B coding region generates three variant isoforms (UNC-49B.1–3) that differ in the intracellular loop between M3 and M4 (see Materials and Methods).

UNC-49C

Two isoforms of UNC-49C were isolated. One encodes a normal full-length subunit, whereas the other, UNC-49Cshort, encodes an unusual subunit truncated at its N terminus.

We did not isolate cDNA species encoding chimeric subunits containing sequences derived from more than one C-terminal repeat. Because we analyzed a large number of clones (see Materials and Methods), we conclude that these are not produced.

Northern blot analysis of poly(A^+) mRNA isolated from *C. elegans* hermaphrodites confirmed that each of the major classes of *unc-49* mRNA is produced (Fig. 1*C*). Intense bands corresponding to the UNC-49B, UNC-49B′, UNC-49C, and UNC-49Cshort mRNA species were detected. UNC-49A-specific bands also were detected, although they were very faint. In addition, a number of large RNAs were identified that may represent splicing intermediates (see *asterisks*, Fig. 1*C*). Quantitative analysis of this Northern blot revealed that UNC-49B and UNC-49C mRNA are present at approximately equal levels, whereas the UNC-49Cshort mRNA is twofold less abundant, UNC-49B′ is fourfold less abundant, and UNC-49A mRNA is 35-fold less abundant (see Materials and Methods).

The UNC-49A, UNC-49B, and UNC-49C subunits share considerable structural overlap. The first 188 identical N-terminal residues are identical among these three subunits (Fig. 2). However, the C termini, which contain most of the known determinants of subunit function, are encoded by different sets of exons. UNC-49C and UNC-49Cshort also share extensive structural overlap. UNC-49Cshort is identical to the C-terminal portion of UNC-49C except for the four amino acids at the N terminus of UNC-49Cshort (Fig. 2).

Structural features of the GABA receptor subunits encoded by *unc-49*

Because *unc-49* encodes three full-length subunits, we speculated that the UNC-49 subunits may be the *C. elegans* homologs of the α, β, and γ subunits of vertebrate $GABA_A$ receptors. To evaluate whether the UNC-49 subunits are closely related to the vertebrate subunits, we performed phylogenetic comparisons by using a comprehensive set of ligand-gated chloride channel subunits. This analysis demonstrated that the UNC-49 subunits are not orthologous to any of the vertebrate $GABA_A$ receptor subunit classes but

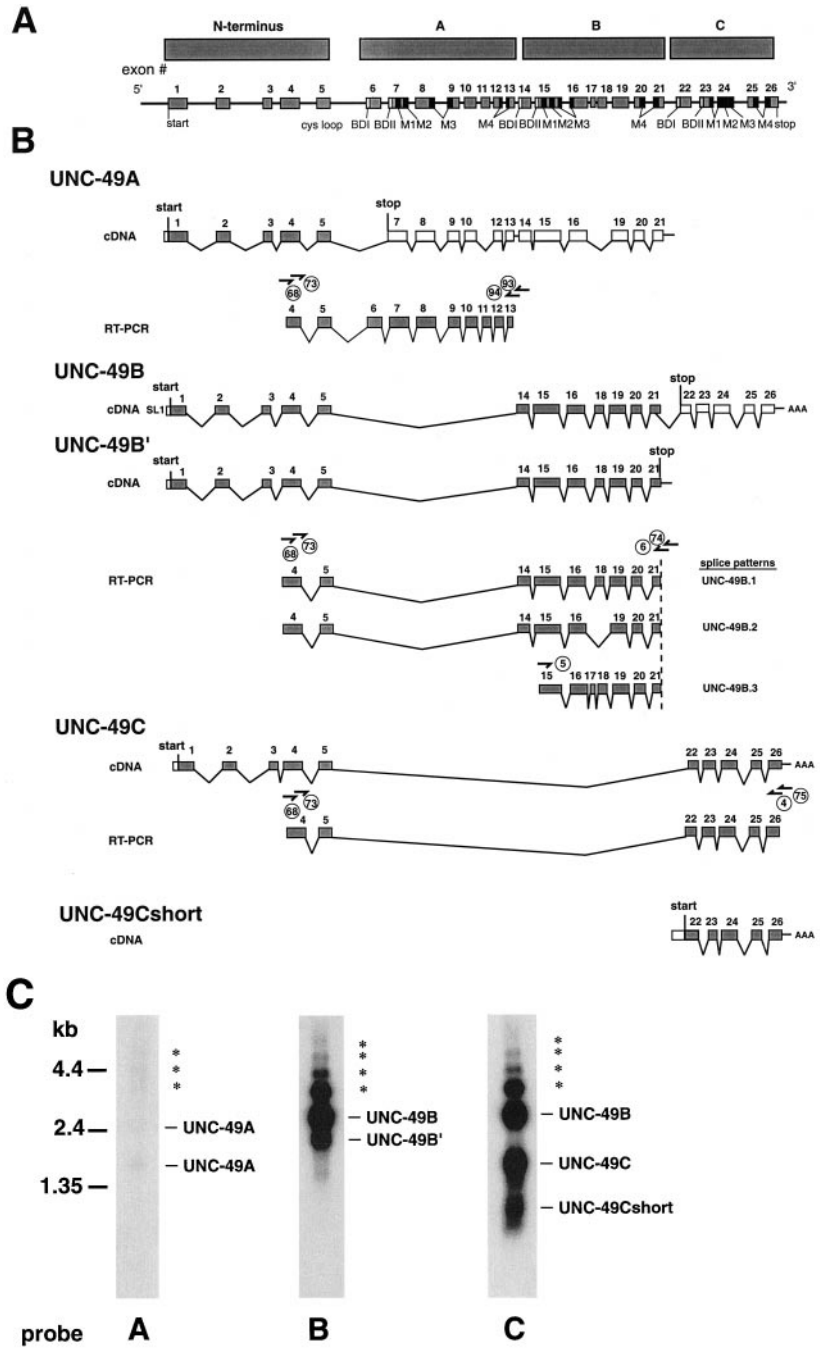

Figure 1. *unc-49* produces three distinct GABA receptor subunits. *A*, Structure of the *unc-49* locus showing the positions of conserved GABA receptor structural motifs. Domain structure of the locus is indicated by *bars* at the *top* (see Results). *B*, *unc-49* mRNA structure. Transcripts were isolated both from cDNA libraries and from RT-PCR experiments. Multiple UNC-49A cDNA clones were identified with different splicing patterns, all resulting in premature stops. One representative example is shown here. Properly spliced RNAs were identified by RT-PCR; the *short arrows* and *circled numbers* represent PCR primers. Two *superimposed* primers (for example, 68 and 73) represent a set of nested PCR primers. The *shaded boxes* represent coding exons, and the *open boxes* represent untranslated regions. The SL1 splice leader was found at the 5′ ends of the mRNA species where indicated. *C*, Northern analysis of poly(A^+) RNA. The probes, indicated *below* each lane, correspond to the C-terminal repeats. Labels to the *right* of each lane indicate the probable identity of each band. In the UNC-49C lane the UNC-49B mRNA is visible because it contains the UNC-49C open reading frame in its 3′ UTR. *Asterisks* indicate higher molecular weight bands that may correspond to partially spliced *unc-49* pre-mRNA. All lanes were exposed for the same length of time.

more closely resemble the *Drosophila melanogaster rdl* gene product (Fig. 3*A*). Because the UNC-49 proteins share a common N terminus, they are grouped into a closely related family. To eliminate this bias from our analysis, we aligned only the C-terminal segments of the ligand-gated chloride channels. The results (data not shown) were primarily the same as those using full-length subunits except that UNC-49C, which is very divergent, forms a unique subunit class.

The results of this phylogenetic analysis imply that the vertebrate α, β, and γ GABA receptor subunit classes arose after the divergence of vertebrates and nematodes. Alternatively, *unc-49* may represent an unusual subunit class while other *C. elegans* genes encode the α, β, and γ subunit homologs. To distinguish between these possibilities, we examined the entire *C. elegans* genome for potential homologs of vertebrate GABA receptor subunits. On the basis of sequence similarity, two of the 30–40 *C. elegans* ligand-gated chloride channel subunits were likely to be GABA receptor subunits. One of these, ZC482.1, is a β-like subunit and the other, F11H8.2, is similar to UNC-49 and *Drosophila rdl* (data not shown). No *C. elegans* subunits were homologous to the vertebrate α and γ GABA receptor subunits.

Sequence comparisons showed strong conservation between the UNC-49 subunits and other ligand-gated chloride channels. However, sequence differences are present in the GABA-binding domains (Fig. 3*B*). The pore-lining M2 region of UNC-49C also contains many nonconserved amino acids (Fig. 3*B*). Nonetheless, we predict that UNC-49C will form a chloride-selective channel because the residues within the channel pore known to affect ion

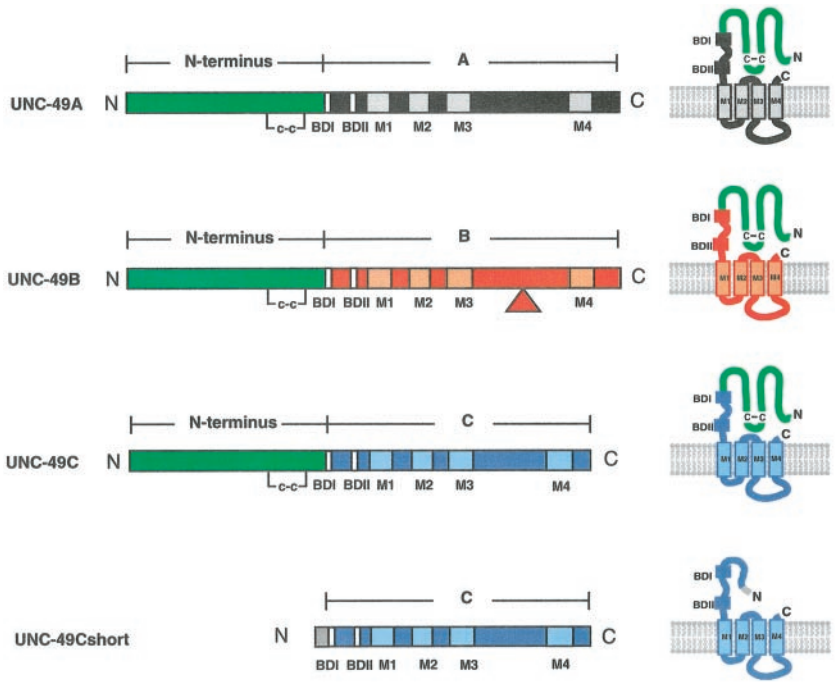

Figure 2. Structural overlap among *unc-49* subunits. UNC-49A, UNC-49B, and UNC-49C are identical over the N-terminal 40% of their length, but they contain different putative GABA-binding domains and transmembrane domains. The *left panel* shows an alignment of each subunit mRNA (the *bar* at the *top* indicates the origin of exons encoding each portion). The *triangle* indicates the position of the alternative splice site in UNC-49B. Note that the UNC49Cshort subunit is identical to the unique C-terminal portion of UNC-49C but that it lacks the entire N terminus common to the other subunits; in its place are four unique N-terminal amino acids (*gray box*). The *right panel* depicts the predicted *unc-49* subunit proteins.

selectivity are conserved (Galzi et al., 1992). Finally, the intracellular loops of the UNC-49 subunits are typical of ligand-gated chloride channel subunits in that they contain several potential protein kinase A, protein kinase C, and casein kinase II phosphorylation sites (Fig. 3*C*). Surprisingly, none of the consensus phosphorylation sites within the UNC-49B intracellular loop is affected by the alternative splicing within this domain (Fig. 3*C*). This finding is unexpected because the numbers of phosphorylation sites in the vertebrate $\beta 2$ and $\gamma 2$ $GABA_A$ receptor subunits are regulated by alternative splicing (Machu et al., 1993; McKinley et al., 1995).

Only UNC-49B is essential for receptor function

Although *unc-49* encodes multiple subunits, an analysis of *unc-49* mutations indicated that only UNC-49B is essential for receptor function. First, *inter se* crosses between all alleles determined that there is only a single complementation group within the *unc-49* locus. Second, all mutant alleles disrupt the UNC-49B subunit. The *n1324, e407*, and *n2392* alleles affect the common N terminus shared by the three full-length subunits (Fig. 4). *unc-49(e407)* is a likely null allele because it contains a premature stop codon in this common region. By contrast, the *e929, e382, e468*, and *e641* alleles disrupt UNC-49B specifically. Three of these, *e382, e468*, and *e641*, contain a charged residue in place of a highly conserved glycine residue within the putative GABA-binding domain BDI (Fig. 4). We confirmed that the mutations within the UNC-49B coding region are responsible for the shrinker phenotype by demonstrating that the UNC-49B open reading frame is required for rescue. Specifically, a construct spanning the entire *unc-49* gene was not capable of rescuing *unc-49(e382)* when an inactivating mutation was introduced specifically into the UNC-49B open reading frame. However, this same construct was capable of rescuing *unc-49(e382)* if an inactivating mutation was introduced into either the UNC-49A or UNC-49C open reading frames, leaving the UNC-49B open reading frame intact. Third, UNC-49B does not require UNC-49C to form a functional receptor *in vivo*. We demonstrated that the construct in which the UNC-49C open reading frame had been inactivated was still capable of rescuing the putative null allele *unc-49(e407)*. This result suggests that UNC-49B is sufficient to form a functional GABA receptor at the neuromuscular junction.

UNC-49B and UNC-49C are colocalized at the neuromuscular junction

By analogy with other complex loci in *C. elegans*, we hypothesized that the subunits encoded within the *unc-49* locus are functionally related. One possibility is that the UNC-49 subunits interact directly to form a heteromultimeric GABA receptor. If so, then the UNC-49 subunits should be coexpressed and colocalized within postsynaptic cells. We tested subunit colocalization by inserting the GFP into the large intracellular loop of each subunit in a plasmid encompassing the entire locus. The resulting constructs, UNC-49A::GFP, UNC-49B::GFP, and UNC-49C::GFP, each produce all of the UNC-49 subunits, one of which is tagged with GFP (Fig. 5*A*). These constructs were able to rescue the shrinker phenotype of *unc-49(e382)* mutants. In addition, we introduced a stop codon into the common N-terminal region of the UNC-49C::GFP construct to create an UNC-49Cshort::GFP construct (Fig. 5*A*). This construct encodes a tagged UNC-49Cshort subunit, but it does not encode any full-length UNC-49 subunit and was unable to rescue the shrinker phenotype.

Using these constructs, we demonstrated that UNC-49B and UNC-49C are coexpressed and colocalized. The UNC-49A::GFP and UNC-49Cshort::GFP constructs did not produce detectable GFP fluorescence. Based on the low levels of UNC-49A mRNA detected by Northern analysis, the lack of UNC-49A::GFP expression was not surprising, but the lack of UNC-49Cshort fluorescence was unexpected. We conclude that the UNC-49Cshort mRNA is not translated efficiently in *C. elegans* hermaphrodites. By contrast, transgenic worms carrying the UNC-49B::GFP and UNC-49C::GFP constructs produced very similar patterns of GFP fluorescence. In both cases, fluorescence was detected mainly in the head muscles and body wall muscles on both the dorsal and ventral sides. Within these cells, faint GFP fluores-

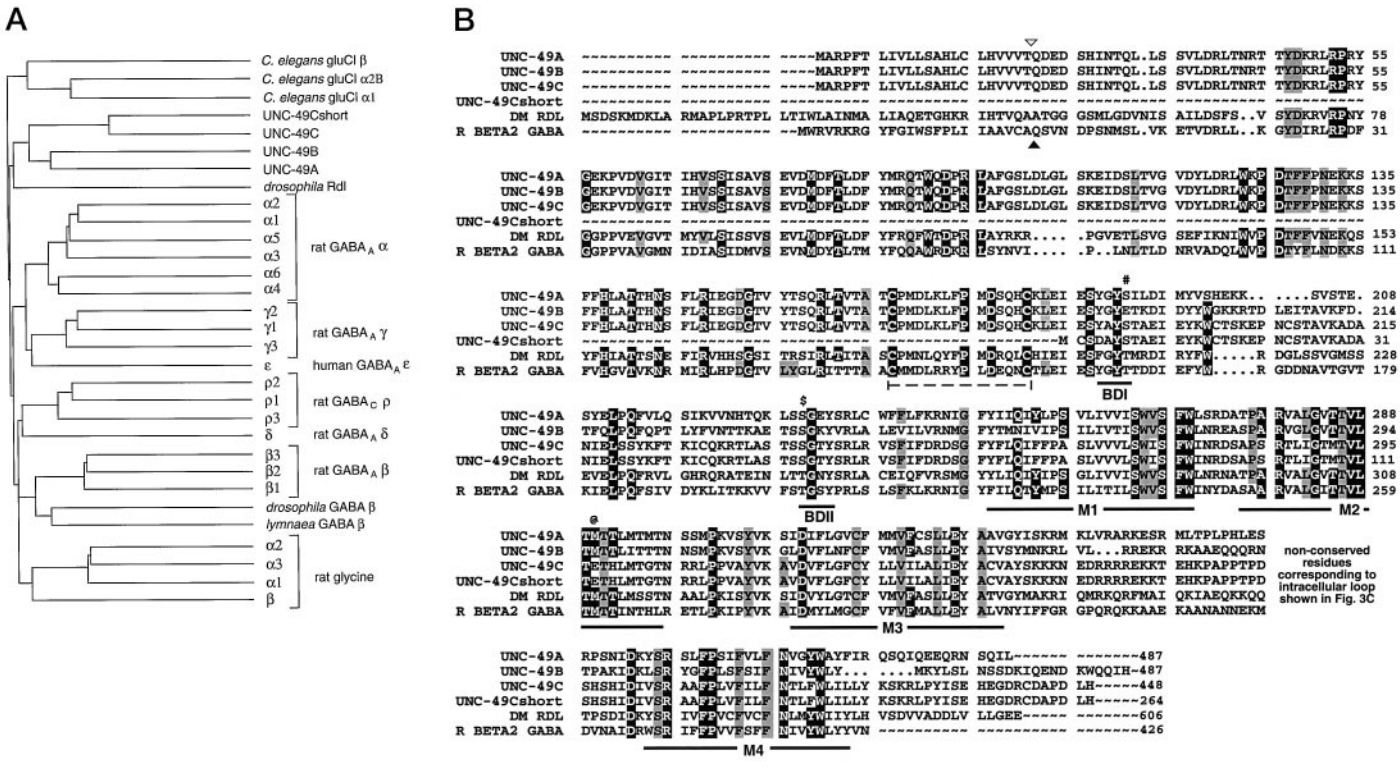

Figure 3. GABA receptor family. *A*, Dendrogram of GABA receptor subunits. The three *unc-49* subunits do not correspond to any of the vertebrate classes of $GABA_A$ receptor subunits. Alignments were performed with the Pileup program in the Genetics Computer Group analysis package. *B*, Sequence alignment of *unc-49* subunits. Residues in *black boxes* are conserved in all members of a set of seven representative non-*C. elegans* GABA receptor subunits, and residues in *gray boxes* are conserved in six of seven members of this set (see Materials and Methods). The rat β2 $GABA_A$ and *Drosophila rdl* receptor subunits are included for comparison. The *dashed line* indicates the disulfide-bonded loop motif ($CX_{13}C$) conserved in all ligand-gated ion channel subunits. The *bars* labeled *BDI* and *BDII* indicate putative GABA-binding domains, and the *bars* labeled *M1–M4* indicate membrane-spanning domains. Residues in BDI and BDII, which are functionally important in the ρ and β GABA receptor subunits but are divergent in the *C. elegans* subunits, are denoted by # and $, respectively. The unusual glutamic acid residue in UNC-49C M2 is denoted by @. *Arrowheads* indicate predicted sites of signal peptide cleavage for UNC-49B and UNC-49C and the rat β2 subunit. Residues are numbered from the predicted start of translation, except for the rat β2 subunit, which is numbered from the predicted signal peptide cleavage site according to convention. UNC-49B is numbered according to the UNC-49B.1 sequence. *C*, Residues comprising the M3–M4 intracellular loops of the *unc-49*-encoded subunits. Sequences of the three UNC-49B isoforms are shown also. Intracellular loop sequences have not been aligned. The *symbols* above each intracellular loop indicate potential regulatory phosphorylation sites (*A* indicates a PKA site, *C* indicates a PKC site, and an *asterisk* indicates a CKII site).

cence was observed in the plasma membrane of the cell soma and muscle arms while intense fluorescence was observed where the motor neurons and muscles make contact (Fig. 5*B,C*). This pattern indicates that the GFP-tagged UNC-49B and UNC-49C subunits are localized efficiently to the neuromuscular junctions. The only consistent difference between the two expression patterns was that strong GFP fluorescence was observed in the sphincter muscle in UNC-49B::GFP animals, but not in UNC-49C::GFP animals (Fig. 5*B,C*). Finally, UNC-49B::GFP and UNC-49C::GFP constructs produced variable, weak fluorescence in the neurons of the head ganglia. However, because our constructs are translational fusions, we could not identify these cells. In summary, the expression patterns of UNC-49B::GFP and UNC-49C::GFP demonstrate that these two subunits potentially could form a heteromeric GABA receptor *in vivo*.

UNC-49B and UNC-49C coassemble in heterologous cells

If UNC-49B and UNC-49C function as a heteromultimer *in vivo*, then it should be possible to demonstrate that they coassemble in heterologous cells. We tested coassembly by expressing the UNC-49 subunits individually or in combination in *Xenopus* oocytes and by analyzing them with the two-electrode voltage-clamp technique. UNC-49B.1, when expressed alone, formed a

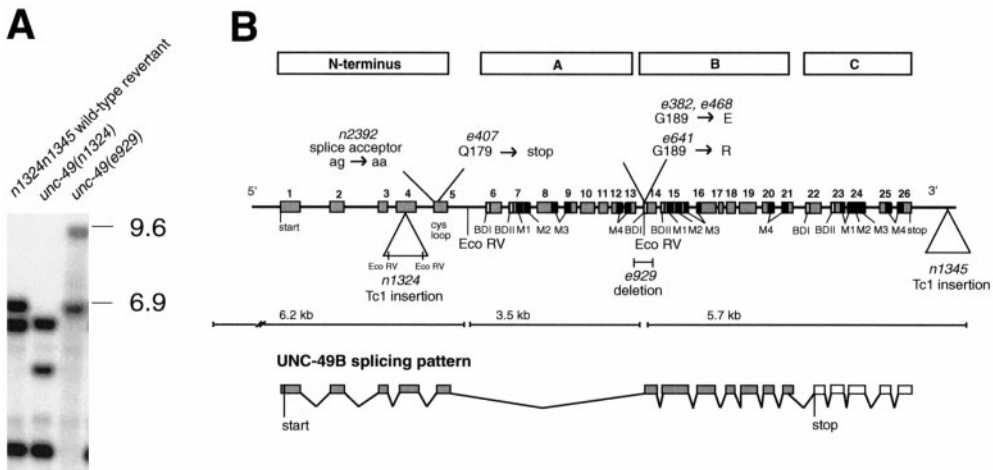

C

allele	mutagen	mutation	protein	subunits affected
e382	EMS	GGG → GAG	G189E	UNC-49B
e407	EMS	CAA → TAA	Q179 stop	UNC-49A, B, C
e468	EMS	GGG → GAG	G189E	UNC-49B
e641	EMS	GGG → AGG	G189R	UNC-49B
e929	^{32}P	small deletion in exon 14	not determined	UNC-49B
n1324	Tc1	Tc1 insertion near exon 4	not determined	UNC-49A, B, C
n1345	*n1324* revertant	excision of n1324 transposon insertion of Tc1 downstream	wild type	none
n2392	EMS	exon 5 splice acceptor G to A	truncation	UNC-49A, B, C

Figure 4. All *unc-49* mutations affect UNC-49B. *A*, Southern blot of *Eco*RV-digested genomic DNA probed with T21C12 insert DNA. The *numbers* at the *right* indicate the positions of DNA size standards. *B*, Positions of mutations in the *unc-49* alleles are shown. *e382*, *e468*, *e641,* and *e929* affect only UNC-49B, whereas *e407*, *n1324*, and *n2392* affect UNC-49A, UNC-49B, and UNC-49C. The *bars* at the *top* represent *unc-49* domains. *C*, Summary of *unc-49* mutations.

homomeric GABA receptor. This receptor produces a robust, desensitizing, dose-dependent current when exposed to GABA (Fig. 6*A*). In a representative experiment the GABA concentration required to produce half-maximal channel activity (EC_{50}) was 43.7 ± 2.9 μM (SEM; $n = 5$), and the Hill coefficient was 2.94 ± 0.28 (SEM; $n = 5$), suggesting that a minimum of three GABA molecules is required to open the channel (Fig. 6*B*). The reversal potential for this current was −30 mV (data not shown), which is consistent with a chloride conductance. UNC-49B receptors are highly GABA-selective. UNC-49B-expressing oocytes did not respond to either glutamate or glycine applied at 1 or 10 mM. Applications of 10 mM β-alanine produced currents that were only slightly greater than baseline noise ($n = 4$; data not shown). By contrast, UNC-49C was not able to form a homomeric GABA receptor. *Xenopus* oocytes injected with UNC-49C RNA failed to respond to GABA at any concentration and were equally unresponsive to glutamate, glycine, and β-alanine. UNC-49A and UNC-49Cshort also were unable to form homomeric GABA receptors.

When UNC-49B and UNC-49C subunits were coexpressed, a functionally distinct receptor was formed. *Xenopus* oocytes were injected with equal amounts of UNC-49B and UNC-49C RNA. The EC_{50} value for GABA on these oocytes was 107.5 ± 13.5 μM (SEM; $n = 5$), and the Hill coefficient was 1.33 ± 0.10 (SEM; $n = 5$; Fig. 6*B*). The GABA dose–response curves were fit accurately with a single Hill equation, which suggests that only a single population of receptors was present. This result indicates that UNC-49B and UNC-49C coassemble very efficiently, such that the homomeric assembly of UNC-49B is eliminated or greatly reduced.

We confirmed that the UNC-49C subunit coassembles efficiently with the UNC-49B subunit by coexpressing these subunits in HEK-293 fibroblast cells and performing single-channel recordings. In cells expressing UNC-49B alone, we observed a single main conductance state of 37.5 ± 2.5 pS (1σ). In cells transfected with UNC-49B and UNC-49C, we observed a single main conductance state of 30.9 ± 2.2 pS (1σ; Fig. 6*C*). We did not observe significant numbers of channel openings corresponding to UNC-49B homomers in cells expressing both UNC-49B and UNC-49C. Although ~10% of channel openings in these cells were larger than the 30.9 pS main conductance, their conductance was approximately twice as large as the main conductance, suggesting that they corresponded to two UNC-49B/C heteromeric channels opening simultaneously. The duration of channel openings also may differ between the two receptors. The UNC-49B homomer appears to remain open longer than the UNC-49B/C heteromer (Fig. 6*C*); however, insufficient numbers of channel openings were analyzed to determine whether these apparent differences are statistically significant. Thus, in HEK-293 cells, like in *Xenopus* oocytes, UNC-49B and UNC-49C coassemble, and the presence of UNC-49C effectively suppresses the homomeric assembly of UNC-49B, suggesting that coassembly is efficient.

DISCUSSION

We cloned the *C. elegans unc-49* gene and demonstrated that it is an unusual complex locus that encodes three GABA receptor subunits by splicing a common N terminus to one of three alternative C termini. Two of these subunits are colocalized to neuromuscular junctions and, in heterologous cells, can assemble to form a heteromultimeric GABA receptor. These results are significant for two reasons. First, the properties of the heteromeric receptor provide insights into the structural basis of GABA receptor function. Second, the use of this complex gene structure to regulate the coexpression of multiple gene products represents a novel genetic regulatory mechanism. This mechanism allows *C. elegans* to coexpress multiple UNC-49 subunits within the same cell and thereby to encode a heteromeric ion channel within a single locus. However, this mechanism also may allow *C. elegans*

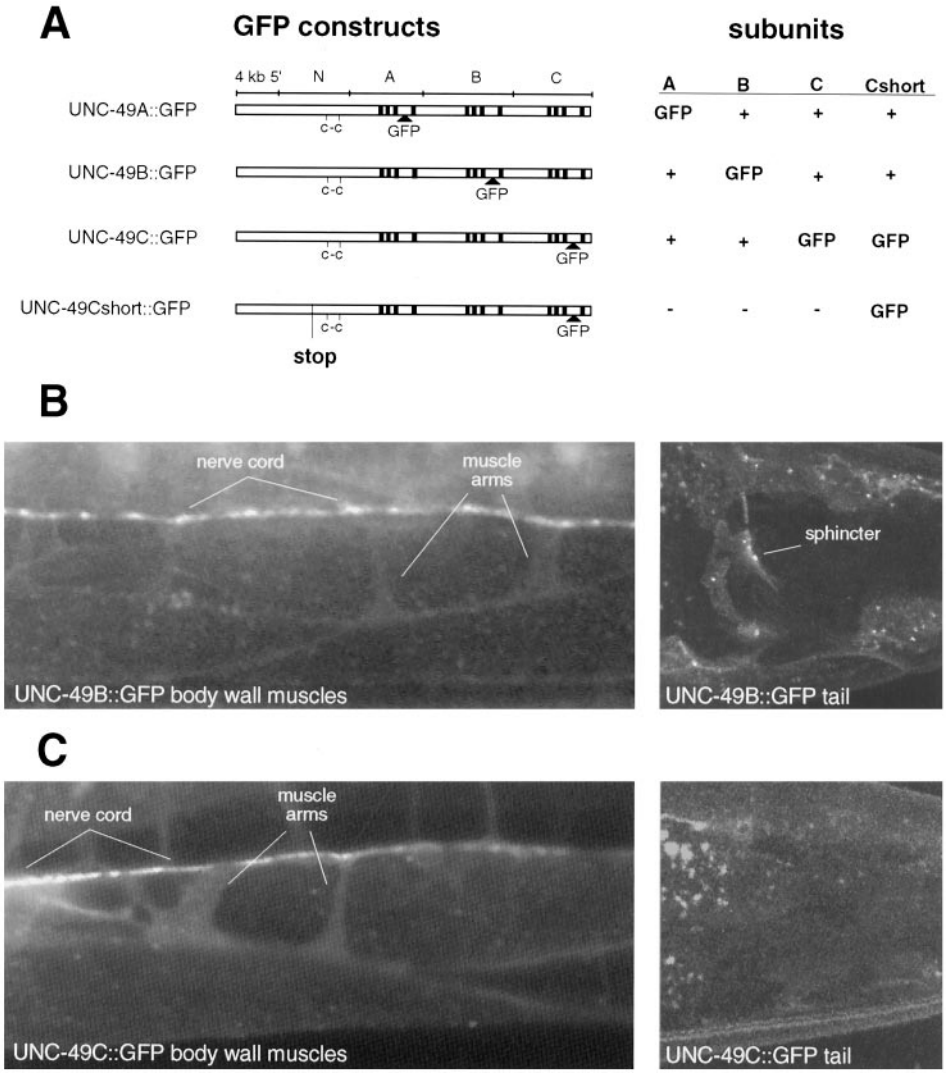

Figure 5. UNC-49B and UNC-49C are coexpressed and colocalized. *A*, Structure of UNC-49::GFP transgenes. The *left panel* shows the site at which GFP was inserted, in frame, into the *unc-49* rescuing fragment. *Vertical bars* represent transmembrane domains. The *right panel* shows the subunits that are produced by the transgene. *GFP* indicates subunits tagged with GFP; + indicates wild-type subunits; − indicates inactivated subunits. *B*, Fluorescence micrographs of UNC-49B::GFP transgenic worms. *Left panel*, Bright GFP fluorescence is visible in a punctate pattern along the nerve cord, where neuromuscular junctions are located. Fainter GFP fluorescence is also visible outlining the muscle cell bodies (lens-shaped bodies beneath the nerve cord) and muscle arms (narrow processes extending from the muscle cell bodies to the nerve cord). *Right panel*, Tail region of an UNC-49B::GFP worm showing bright fluorescence in the sphincter muscle. *C*, Fluorescence micrographs of UNC-49C::GFP transgenic worms. The pattern of fluorescence is similar to that observed in the UNC-49B::GFP transgenic animals in the body wall muscles and nerve cord (*left panel*). However, no fluorescence is visible in the sphincter muscle (*right panel*).

to express UNC-49 subunits differentially in different cells and thereby encode a diverse set of ion channels with a single locus.

Subunit structure and function

Subunits that are structurally and functionally diverse are valuable reagents for studies aimed at identifying the determinants of $GABA_A$ receptor function (see Mihic et al., 1997). Our results so far have led to three insights concerning the structural basis of UNC-49 GABA receptor function.

First, the importance of the putative GABA-binding domain BDI for receptor activation by GABA is conserved between nematodes and vertebrates. Previous structure–function studies have demonstrated that BDI is required for the activation of vertebrate GABA receptors by GABA (Amin and Weiss, 1993, 1994). BDI contains a highly conserved glycine residue that is thought to form a hairpin turn within the ligand-binding pocket. We have demonstrated that the homologous glycine residue within the BDI motif of UNC-49B is mutated to a charged residue in three of the *unc-49* mutant alleles. Animals with these mutations lack GABA receptor function, which indicates that, like vertebrate GABA receptors, the UNC-49 GABA receptor requires BDI for activation by a ligand.

The importance of this domain for receptor activation also is suggested by a more subtle difference within BDI of UNC-49C and BDI of vertebrate GABA receptors. In UNC-49C, a conserved threonine residue in BDI is replaced by a serine. UNC-49C confers decreased GABA sensitivity when it coassembles with UNC-49B. Likewise, in vertebrate GABA receptors, mutating the homologous threonine residue to a serine residue causes reduced GABA sensitivity (Amin and Weiss, 1993, 1994). Although we cannot rule out that the reduced GABA sensitivity of the UNC-49B/C heteromer is attributable to some other UNC-49C residue, it is intriguing that parallel functional effects are observed with both nematode and vertebrate GABA receptor subunits when a serine residue is present at this position. Our interpretation is that UNC-49C represents a naturally occurring subunit variant that supports the role of the BDI domain in the activation of the channel by GABA. If so, it is significant that the serine residue in UNC-49C exerts its effects in the context of a wild-type subunit. In a mutagenized subunit the effects of any amino acid change might reflect a nonspecific perturbation of subunit secondary structure rather than indicate a specific role for that amino acid in the function of the receptor. To observe a structural and functional parallel in a wild-type subunit argues for a specific effect because the secondary structure of a wild-type subunit is, necessarily, intact. The functional parallels between the mutagenized vertebrate subunits and UNC-49C therefore

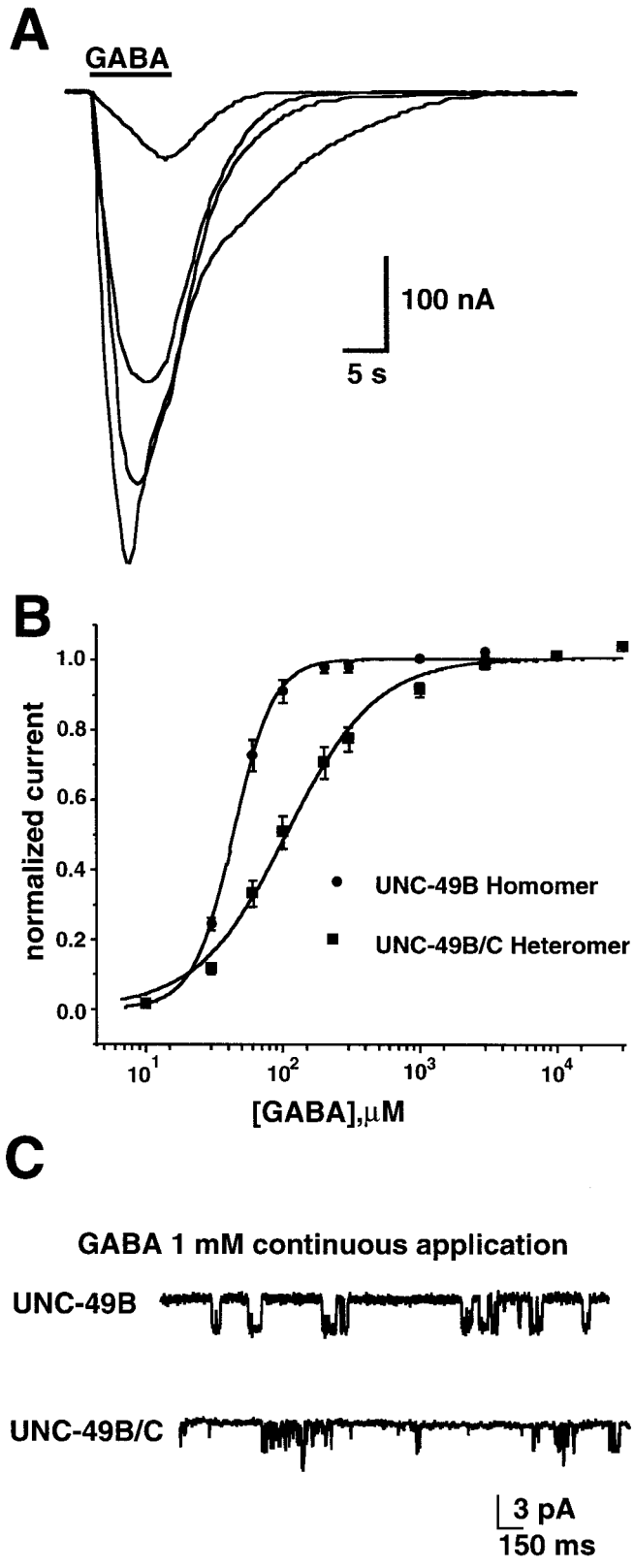

Figure 6. UNC-49B and UNC-49C coassemble in heterologous cells. *A*, Response of a representative UNC-49B.1-injected oocyte to 10 sec pulses of GABA at 10, 30, 60, and 100 μM. *B*, GABA dose–response curves obtained from *Xenopus* oocytes injected with UNC-49B (*circles*) or UNC-49B plus UNC-49C (*squares*). Error bars represent SEM. *C*, Single-channel recordings from HEK-293 cells expressing UNC-49B alone (*top trace*) or UNC-49B plus UNC-49C (*bottom trace*).

strengthen the conclusion that the threonine residue in BDI of the vertebrate subunits plays a specific role in receptor activation by GABA.

Second, we propose that a negatively charged residue within the pore-lining M2 domain of UNC-49C is an important determinant of the pore properties of the UNC-49B/C heteromeric GABA receptors. The addition of UNC-49C to the UNC-49B GABA receptor resulted in reduced chloride conductance. A parallel effect has been described for the glycine receptor β-subunit. This subunit contains a glutamic acid residue within the M2 domain that causes α/β heteromers to display reduced single-channel conductance as compared with glycine α-homomers (Bormann et al., 1993). Our data suggest that the glutamic acid residue in UNC-49C plays an analogous role, although it is possible that other UNC-49C residues contribute to the reduced conductance of the UNC-49B/C heteromeric receptor. These data raise the possibility that vertebrates and nematodes use common mechanisms to regulate the pore properties of ligand-gated anion channels, namely, that a subunit with a negatively charged residue in its pore-lining domain can be added to a receptor to reduce its conductance.

Finally, the structural overlap among UNC-49A, UNC-49B, and UNC-49C suggests that the N-terminal part of a GABA receptor subunit exhibits some degree of autonomy with respect to protein folding and function. In other words, the shared N-terminal domain can fold and function whether it is fused to the UNC-49A, UNC-49B, or UNC-49C C terminus.

It is puzzling that UNC-49C does not appear to be required for receptor function *in vitro* or *in vivo*. Four observations argue against a necessary role of UNC-49C. (1) Electrophysiological data indicate that UNC-49B can form a functional GABA receptor in the absence of UNC-49C *in vitro*. (2) UNC-49B is sufficient to rescue the shrinker phenotype of *unc-49* mutants in the absence of UNC-49C. (3) None of *unc-49* mutant alleles lacked UNC-49C specifically. (4) In one cell, UNC-49B appears to be expressed in the absence of UNC-49C. At present, the role of UNC-49C *in vivo* is not clear. It is possible that in *C. elegans*, optimally efficient locomotion requires inhibitory postsynaptic currents with very precisely defined rise times, maximal amplitudes, and decay kinetics. The UNC-49C subunit could exert a subtle influence on these properties, which confers a selective advantage in the wild but cannot be detected by visual observation of animals in the laboratory. Alternatively, UNC-49C might alter the pharmacological properties of the GABA receptor to allow for allosteric modulation or to confer resistance to toxins present in the environment.

The *unc-49* gene structure and its implications for GABA receptor structure

The gene structure of *unc-49* is distinct from the structures of multi-gene arrangements previously described in *C. elegans*. One common multi-gene arrangement in *C. elegans* is the operon, in which genes are arranged tandemly and transcribed as a single pre-mRNA under the control of a single promoter. Subsequent trans-splicing steps separate the mRNA molecules that then are translated independently (Blumenthal and Steward, 1997). Another type of arrangement is observed in the *cha-1–unc-17* compound locus. These two genes encode choline acetyltransferase and the vesicular acetylcholine transporter, respectively. *cha-1* and *unc-17* share a promoter and a single noncoding exon, which is spliced either to a set of CHA-1-encoding exons or to a set of UNC-17-encoding exons (Alfonso et al., 1994). A similar ar-

rangement was reported for *unc-60*, which encodes two distinct actin depolymerizing proteins (McKim et al., 1994). *unc-49,* along with another recently described ligand-gated chloride channel subunit locus (Laughton et al., 1997), defines a third type of multi-gene organization in which common 5′ exons are spliced to tandem alternative copies of 3′ exons.

The *unc-49* gene structure has two major implications for the subunit composition of *C. elegans* GABA receptors. Specifically, this gene structure can allow for the coordinate regulation of subunits in the *same* cells or the differential regulation of subunits in *different* cells.

Multi-gene arrangements in *C. elegans* facilitate the coordinate regulation of multiple proteins in the same cells, and these proteins often function together in a biochemical or developmental pathway (Blumenthal and Steward, 1997). Our results show that *unc-49* behaves according to this general rule. Two of the UNC-49 subunits are coexpressed in the same cells, colocalize to synaptic regions within those cells, and can coassemble efficiently into a heteromeric GABA receptor. Together, these data strongly suggest that UNC-49B and UNC-49C form a heteromeric GABA receptor *in vivo.* Thus, the first major implication of the *unc-49* gene organization is that it allows *C. elegans* to encode a heteromultimeric ion channel using a single locus.

The second implication of the *unc-49* gene structure is that *C. elegans* may be able to encode a diverse set of GABA receptors in different cells using a single locus. For example, most muscles that express UNC-49B::GFP also express UNC-49C::GFP. However, the sphincter muscle expresses only UNC-49B::GFP; therefore, this cell may use an UNC-49B homomer. Alternatively, it is possible that the difference between the UNC-49B and UNC-49C expression patterns reflects differential expression of the transgenes in extrachromosomal arrays. However, we believe that this is a less likely explanation because multiple independent transgenic lines showed differential expression of UNC-49B::GFP and UNC-49C::GFP, and the structure of the two transgenes is identical apart from the positioning of the GFP coding sequences. UNC-49A may represent another example of differential expression of UNC-49 subunits. UNC-49A subunit expression could not be detected in hermaphrodites, whereas UNC-49B and UNC-49C are expressed at high levels. Although it is possible that UNC-49A is a recent pseudogene with no physiological function, the conservation of the UNC-49A open reading frame implies that, under some circumstances, UNC-49A plays a role.

The coordinate regulation of subunit expression is a prerequisite for producing heteromeric ion channels. In vertebrates, each ion channel subunit is encoded by a separate gene. The promoters of some of these genes share functional similarities that allow for the coexpression of multiple different subunits in the same cell and thus permit the formation of heteromeric receptors. However, subunit expression patterns are not identical, so different cells express different sets of receptors. By contrast, *C. elegans* expresses subunits in the same cells or in different cells, using a single promoter. Coexpression of UNC-49B and UNC-49C in the body muscles is achieved by splicing to the B or C transmembrane domain regions equally. Expression in different cells presumably is achieved by using these splice patterns differentially. Thus, by regulating mRNA splicing, *C. elegans* can produce different receptor types using a single locus.

REFERENCES

Alfonso A, Grundahl K, McManus JR, Asbury JM, Rand JB (1994) Alternative splicing leads to two cholinergic proteins in *Caenorhabditis elegans*. J Mol Biol 241:627–630.

Amin J, Weiss DS (1994) Homomeric ρ1 GABA channels: activation properties and domains. Receptors Channels 2:227–236.

Amin J, Weiss DS (1993) $GABA_A$ receptor needs two homologous domains of the beta-subunit for activation by GABA but not by pentobarbital. Nature 366:565–569.

Andres AJ, Thummel CS (1994) Methods for quantitative analysis of transcription in larvae and prepupae. Methods Cell Biol 44:565–573.

Ausubel FM, Brent R, Kingston RE, Moore DD, Seidman JG, Smith JA, Struhl K (1995) Current protocols in molecular biology. New York: Wiley.

Barstead RJ, Waterston RH (1989) The basal component of the nematode dense-body is vinculin. J Biol Chem 264:10177–10185.

Blumenthal T, Steward K (1997) RNA processing and gene structure. In: *C. elegans* II (Riddle DL, Blumenthal T, Meyer BJ, Priess JR, eds), pp 117–145. Cold Spring Harbor, NY: Cold Spring Harbor Laboratory.

Bormann J, Rundstrom N, Betz H, Langosch D (1993) Residues within transmembrane segment M2 determine chloride conductance of glycine receptor homo- and hetero-oligomers. EMBO J 12:3729–3737.

Clark SG, Lu X, Horvitz HR (1994) The *Caenorhabditis elegans* locus *lin-15*, a negative regulator of a tyrosine kinase signaling pathway, encodes two different proteins. Genetics 137:987–997.

Donevan SD, Beg A, Gunther JM, Twyman RE (1998) The methylglutamate, SYM 2081, is a potent and highly selective agonist at kainate receptors. J Pharmacol Exp Ther 285:539–545.

Feinberg AP, Vogelstein B (1983) A technique for radiolabeling DNA restriction endonuclease fragments to high specific activity. Anal Biochem 132:6–13.

Galzi JL, Changeux JP (1994) Neurotransmitter-gated ion channels as unconventional allosteric proteins. Curr Opin Struct Biol 4:554–565.

Galzi JL, Devillers-Thiery A, Hussy N, Bertrand S, Changeux JP, Bertrand D (1992) Mutations in the channel domain of a neuronal nicotinic receptor convert ion selectivity from cationic to anionic. Nature 359:500–505.

Laughton DL, Lunt GG, Wolstenholme AJ (1997) Alternative splicing of a *Caenorhabditis elegans* gene produces two novel inhibitory amino acid receptor subunits with identical ligand binding domains but different ion channels. Gene 201:119–125.

Lavoie AM, Tingey JJ, Harrison NL, Pritchett DB, Twyman RE (1997) Activation and deactivation rates of recombinant $GABA_A$ receptor channels are dependent on α-subunit isoform. Biophys J 73:2518–2526.

Macdonald RL, Olsen RW (1994) $GABA_A$ receptor channels. Annu Rev Neurosci 17:569–602.

Machu TK, Firestone JA, Browning MD (1993) Ca^{2+}/calmodulin-dependent protein kinase II and protein kinase C phosphorylate a synthetic peptide corresponding to a sequence that is specific for the γ2L subunit of the $GABA_A$ receptor. J Neurochem 61:375–377.

McIntire SL, Jorgensen E, Horvitz HR (1993a) Genes required for GABA function in *Caenorhabditis elegans*. Nature 364:334–337.

McIntire SL, Jorgensen E, Kaplan J, Horvitz HR (1993b) The GABAergic nervous system of *Caenorhabditis elegans*. Nature 364:337–341.

McKernan RM, Whiting PJ (1996) Which $GABA_A$ receptor subtypes really occur in the brain? Trends Neurosci 19:139–143.

McKim KS, Matheson C, Marra MA, Wakarchuk MF, Baillie DL (1994) The *Caenorhabditis elegans unc-60* gene encodes proteins homologous to a family of actin-binding proteins. Mol Gen Genet 242:346–357.

McKinley DD, Lennon DJ, Carter DB (1995) Cloning, sequence analysis, and expression of two forms of mRNA coding for the human β2 subunit of the $GABA_A$ receptor. Brain Res Mol Brain Res 28:175–179.

Mello CC, Kramer JM, Stinchcomb D, Ambros V (1991) Efficient gene transfer in *C. elegans*: extrachromosomal maintenance and integration of transforming sequences. EMBO J 10:3959–3970.

Meyer G, Kirsch J, Betz H, Langosch D (1995) Identification of a gephyrin binding motif on the glycine receptor beta subunit. Neuron 15:563–572.

Mihic SJ, Ye Q, Wick MJ, Koltchine VV, Krasowski MD, Finn SE, Mascia MP, Valenzuela CF, Hanson KK, Greenblatt EP, Harris RA,

Harrison NL (1997) Sites of alcohol and volatile anaesthetic action on $GABA_A$ and glycine receptors. Nature 389:385–389.

Moss SJ, Smart TG (1996) Modulation of amino acid-gated ion channels by protein phosphorylation. Int Rev Neurobiol 39:1–52.

Nusser Z, Sieghart W, Somogyi P (1998) Segregation of different $GABA_A$ receptors to synaptic and extrasynaptic membranes of cerebellar granule cells. J Neurosci 18:1693–1703.

Okkema PG, Fire A (1994) The *Caenorhabditis elegans* NK-2 class homeoprotein CEH-22 is involved in combinatorial activation of gene expression in pharyngeal muscle. Development 120:2175–2186.

Olsen RW, Tobin AJ (1990) Molecular biology of $GABA_A$ receptors. FASEB J 4:1469–1480.

Rodriguez IR, Mazuruk K, Schoen TJ, Chader GJ (1994) Structural analysis of the human hydroxyindole-*O*-methyltransferase gene. Presence of two distinct promoters. J Biol Chem 269:31969–31977.

Wilson R, Ainscough R, Anderson K, Baynes C, Berks M, Bonfield J, Burton J, Connell M, Copsey T, Cooper J, Coulson A, Craxton M, Dear S, Du Z, Durbin R, Favello A, Fraser A, Fulton L, Gardner A, Green P, Hawkins T, Hillier L, Jier M, Johnston L, Jones M, Kershaw J, Kirsten J, Laisster N, Latreille P, Lightning J, Lloyd C, Mortimore B, O'Callaghan M, Parsons J, Percy C, Rifken L, Roopra A, Saunders D, Shownkeen R, Sims M, Smaldon N, Smith A, Smith M, Sonnhammer E, Staden R, Sulston J, Thierry-Mieg J, Thomas K, Vaudin M, Vaughan K, Waterston R, Watson A, Weinstock L, Wilkinson-Sproat J, Wohldman P (1994) 2.2 Mb of contiguous nucleotide sequence from chromosome III of *C. elegans.* Nature 368:32–38.